High-order harmonic generation in laser-aligned molecules

N. Hay,[1,*] R. Velotta,[1,†] M. Lein,[1] R. de Nalda,[1] E. Heesel,[1] M. Castillejo,[2] and J. P. Marangos[1]
[1]*The Blackett Laboratory, Imperial College of Science, Technology and Medicine, London SW7 2BW, United Kingdom*
[2]*Instituto de Química-Física Rocasolano, CSIC, Serrano 119, 28006 Madrid, Spain*
(Received 21 December 2001; published 19 April 2002)

We demonstrate high-order harmonic generation in high-density vapors of laser-aligned molecules. Ensembles of aligned CS_2 and N_2 are formed in the focus of a 300 ps duration laser pulse with sufficient density ($\sim 10^{17}$ molecules cm^{-3}) to enable efficient high-order harmonic generation by a second, 70-fs, high-intensity laser pulse. We are able to modulate and significantly enhance the harmonic intensity in aligned molecules compared to the randomly oriented case. Our results are explained by considering the influence of an anisotropic dipole phase. Strong support for this interpretation is provided by theoretical results for high-order harmonic generation in the aligned H_2^+ model system.

DOI: 10.1103/PhysRevA.65.053805 PACS number(s): 42.65.Ky, 42.50.Vk, 33.80.Rv

I. INTRODUCTION

High-order harmonic generation (HHG) resulting from the interaction of intense laser light with atoms has been extensively studied in recent years as a unique source of coherent XUV radiation [1]. An intuitive and durable theoretical picture based on the classical electron trajectory in the laser field has helped to elucidate this process [2]. Several workers have observed the similarity of HHG in atoms and small molecules [3,4], and recently it was shown that if sufficiently short pulses are used ($<$100 fs) then even larger (organic) molecules exhibit atomlike behavior [5]. However, unlike atoms, molecules are not isotropic systems. It is known that processes such as multiphoton ionization can be strongly influenced by the angle between the laser electric-field vector and the molecular axis [6], and it is, therefore, natural to ask if there is any orientation dependence of the closely related process of HHG. This question is addressed in a theoretical paper in which it was shown that the amplitude of the single-molecule HHG response in a H_2^+ ion is increased if the laser field is polarized perpendicular to the molecular axis [7]. Our experimental results confirm that the HHG yield can indeed be increased in an aligned molecular medium [8]. However, these results strongly suggest that modifications to the *phase* of the single-molecule response can be the dominant influence of molecular alignment. This anisotropic dipole phase has been investigated in recent theoretical work [9] that is considered here.

To study experimentally how HHG depends upon molecular orientation it is first necessary to align a dense ($>10^{17}$ cm^{-3}) ensemble of molecules. Alignment has been demonstrated at low densities ($\sim 10^{10}$ cm^{-3}) for molecules having no permanent dipole moment [10,11] where the electric field of a laser pulse simultaneously induces a molecular dipole moment and exerts a torque upon it [12]. Under the conditions discussed below, this torque creates an ensemble of molecules with an angular distribution of molecular axes that is peaked about the direction of the electric field. From the quantum-mechanical point of view, the eigenstates of aligned molecules in the adiabatic limit correspond to the so-called pendular states and can be labeled by the quantum numbers $\tilde{J}$ and M of the field-free rotational state [13]. The degree of alignment is quantified by the expectation value of $\cos^2\theta$, $\langle\cos^2\theta\rangle$, where θ is the angle between the molecular axis and the electric-field vector. It ranges from $\frac{1}{3}$, corresponding to no alignment, to 1 when the molecule is in a perfectly aligned state along the electric-field vector. For an ensemble of molecules in thermal equilibrium, the average of the Boltzmann distribution of the rotational states has also to be considered; thus we have [10,13]

$$\langle\cos^2\theta\rangle = \sum_{\tilde{J}} w_{\tilde{J}} \sum_{M=-\tilde{J}}^{M=+\tilde{J}} \langle\cos^2\theta\rangle_{\tilde{J},M}. \quad (1)$$

In Eq. (1), $\langle\cos^2\theta\rangle_{\tilde{J},M}$ is the expectation value of $\cos^2\theta$ over the rotational state characterized by the quantum numbers $\tilde{J}$ and M and $w_{\tilde{J}} = \exp[-\tilde{J}(\tilde{J}+1)/\gamma]/Q_r$, where Q_r is the rotational partition function and $\gamma = kT/B$ is the reduced rotational temperature (B is the rotational constant of the molecule). In [11], asymptotic expressions for $\langle\cos^2\theta\rangle_{\tilde{J},M}$ are reported as a function of the anisotropy parameter $c = (\omega_\parallel - \omega_\perp)^{1/2}$, where $\omega_{\parallel,\perp} = \alpha_{\parallel,\perp} {E_0}^2/4B$, where $\alpha_\parallel$ and $\alpha_\perp$ are the parallel and normal polarizabilities of the molecule and E_0 is the electric-field amplitude.

In earlier work [10,14–16], a $\approx$3.5 ns duration laser pulse was used to align several species of neutral molecules in samples of density $<10^{10}$ cm^{-3}, and a degree of alignment as high as $\langle\cos^2\theta\rangle = 0.9$ was realized.

In this paper, we present results from the study of HHG in dense vapors of spatially aligned molecules. To our knowledge this is the first time that controlled alignment has been demonstrated at densities as high as 10^{17} cm^{-3}. We show that HHG may be enhanced and modulated by controlled alignment of the molecules in a nonlinear medium. The results of both experiment and numerical calculation lead us to conclude that it is the highly anisotropic phase of the strongly driven molecular dipole that dominates the observed behavior.

*Corresponding author. Email address: n.hay@ic.ac.uk
†Present address: Istituto Nazionale Fisica della Materia, Dipartimento Scienze Fisiche, Via Cintia, 26-80126-Napoli, Italy.

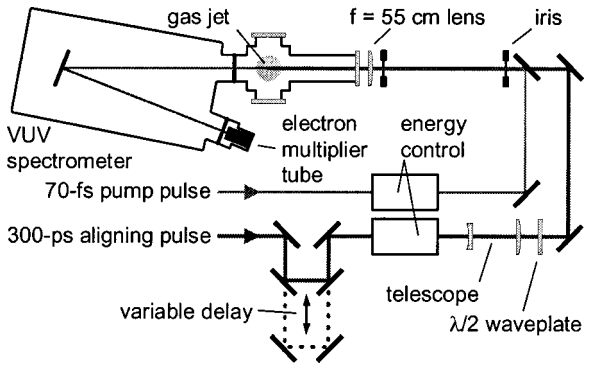

FIG. 1. Experimental setup showing 300 ps duration alignment laser pulses and 70 fs duration high-order harmonic generation pump pulses focused collinearly into a dense molecular gas jet.

II. EXPERIMENT

A. Laser system and optics

Our experimental arrangement is shown in Fig. 1. A Ti: sapphire, chirped pulse amplification laser system with center wavelength 798 nm and repetition rate 10 Hz was used to simultaneously produce 300 ± 30 ps duration laser pulses for molecular alignment and (70 ± 5)-fs laser pulses to pump HHG in the aligned molecules. A beam splitter immediately before the grating pulse compressor divided the linearly polarized laser pulse into two parts. The reflected fraction propagated through a beam expanding telescope into the pulse compressor to produce 70 fs full width at half maximum (FWHM) duration, 40-mJ pump pulses. The transmitted fraction remained uncompressed to provide laser pulses for control of molecular alignment with 300 ps FWHM duration and energy up to 60 mJ.

To synchronize the aligning and pump pulses, the aligning pulses passed through a fixed optical delay of path length equivalent to the pulse compressor. An additional delay was introduced by a retroreflector mounted on a high-resolution translation stage to control the relative delay between the two pulses, Δt with <100 fs resolution over a range of 700 ps. The retroreflector position corresponding to zero delay, $\Delta t=0$, was determined with an accuracy of ±50 ps by monitoring separately the arrival time of the aligning and pump pulses using a fast photodiode (Thorlabs DET210) and digital oscilloscope (Tektronics TDS680B). The energy of the harmonic pump pulses was controlled by rotating a λ/2 wave plate placed before the pulse compressor, which had a very strong polarization dependence in its transmission efficiency. A wave plate and a polarizing beam splitter were used to vary the aligning pulse energy. The focused intensities in the interaction region could be varied in the range 5×10^{13}–5×10^{14} W cm^{-2} for the 70-fs HHG pump pulses and 1×10^{11}–2×10^{12} W cm^{-2} for the 300-ps aligning pulses (below the threshold for HHG).

Both the aligning and pump beams were linearly polarized. Control of the molecular alignment plane was achieved by rotating the polarization vector of the aligning beam to be either parallel with or perpendicular to the polarization vector of the pump beam using a λ/2 wave plate.

The aligning beam was modulated at 5 Hz by a mechanical chopper wheel phase locked to the laser pulses to optimize the signal-to-noise ratio of measurements, comparing the harmonic intensity with and without the aligning pulse.

The pump and aligning beams were recombined in a 50:50 beam splitter then aligned through a pair of irises and focused into a small vacuum chamber by a planoconvex fused silica lens with focal length 55 cm. The intensity profiles and spatial overlap of the aligning and pump pulses were measured before and after every experiment. The beams were sampled by an optical wedge inserted after the focusing lens and attenuated by a neutral density filter. The focal volume was then imaged onto a charge-coupled device camera using a microscope objective and sampled by a personal computer (PC) equipped with a frame grabber.

The peak intensities in the aligning and pump beam foci were calculated using measurements of the intensity profiles, pulse energies, and pulse durations. Pulse energies were measured using a laser energy meter (Molectron JMAX43). The duration of the aligning pulse was measured by a fast sampling diode (New Focus 1437). We used a second-order single-shot autocorrelator to measure the duration of the pump pulse assuming a sech^2 temporal profile. We estimate a factor of 5 error in the calculated peak intensity.

B. High-order harmonic detection and data acquisition

High-order harmonics generated in the interaction were spectrally resolved using a vacuum ultraviolet monochromating spectrometer (GCA McPherson 225) and detected by an electron multiplier tube (EMT, Electron Tubes 143).

The aligning and pump pulses were derived from the same laser system so that their shot-to-shot energy fluctuations were proportional, and a single photodiode, calibrated by the energy meter, was able to simultaneously monitor the energy fluctuations of both beams.

The signals from the EMT (harmonic intensity) and the photodiode (pulse energy) together with a signal defining the state of the alignment beam (blocked or unblocked) were sampled by the digital oscilloscope and transferred to a PC for immediate analysis. The ratio R of the harmonic intensity with the aligning beam (molecules aligned) to the harmonic intensity without the aligning beam (molecules randomly oriented) was determined. For each datum, the average and the standard error of R were calculated over 400 laser pulses.

C. Gas-jet characteristics

A pulsed molecular jet was produced by a temperature controlled solenoid valve system consisting of integrated heating elements, a sample reservoir, pressure gauge, thermocouple, and pulsed solenoid valve mounted on the vacuum chamber above the laser focus (Fig. 2). For these experiments, the valve was modified to allow helium buffer gas to be bubbled through the liquid sample, thus mixing with the molecular vapor and enhancing rotational cooling of the molecular vapor during its supersonic expansion into vacuum. The laser beam was focused 3 mm below the 500-μm-diameter nozzle to give an interaction region ~6 mm long with density $\sim10^{17}$ molecules cm^{-3}. We estimate the

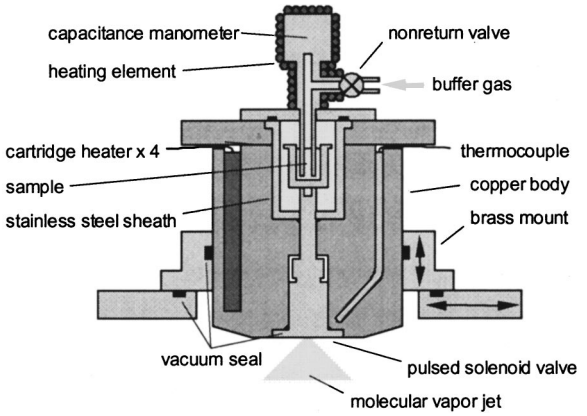

FIG. 2. Temperature controlled pulsed valve with integral sample reservoir and buffer gas supply used to generate high-density, rotationally cooled molecular vapors.

rotational temperature of molecules in the jet [17] to be ≈10 K for CS_2 (350-Torr CS_2 with 1400-Torr He) and ≈25 K for N_2 and H_2. These conditions provided rotational cooling sufficient to allow strong alignment while retaining an acceptable HHG signal-to-noise ratio.

Our estimates of the density and temperature of the molecular jet are obtained using the framework of the theory described by Miller [17]. From the estimated temperature we can calculate the degree of alignment, given the species and the aligning laser intensity. The maximum cooling effect is obtained by locating the interaction region beyond the quitting surface, where the expansion becomes collisionless and the temperature remains constant. However, in order to ensure sufficient gas density for HHG, the interaction region is located close to the nozzle. This position does not realize the maximum cooling effect of the expansion, but is instead a compromise chosen to optimize the signal-to-noise ratio by considering the increased alignment effect at lower temperatures and the increased harmonic intensity at higher density.

The starting point of the determination of the rotational temperature is the evaluation of the terminal speed ratio, i.e., the final value for the ratio between the parallel (∥) mean velocity divided by the thermal spread in velocities. It is given by [17]

$$S_{\parallel,\infty}=A\left[\sqrt{2}n_0 d\left(\frac{53C_6}{kT_0}\right)^{1/3}\right]^B, \tag{2}$$

where A and B are two parameters depending on the ratio of specific-heat capacities γ, n_0 and T_0 are the source gas density (atoms cm^{-3}) and temperature (K), respectively, and d is the nozzle diameter (cm). The quantity C_6 depends on the Lennard-Jones parameters ε and σ through the relation $C_6/k=4(\varepsilon/k)\sigma^6$. For He we have $C_6/k=0.15\times10^{-43}$ K cm^6 whereas for CS_2, $C_6/k=150\times10^{-43}$ K cm^6.

Taking $n_0=5\times10^{19}$ cm^{-3} (1400 Torr) and $d=0.5$ mm, we obtain $S_{\parallel,\infty}\approx35$ for He. From the relation between the speed ratio S and the Mach number M we get the terminal Mach number

$$M_\infty=\sqrt{\frac{2}{\gamma}}S_{\parallel,\infty}\simeq38.5. \tag{3}$$

Once we have M_∞, we can evaluate the distance of the quitting surface from the nozzle, X_q. For $X\gg d$, we have

$$X_q=\left(\frac{M_\infty}{C_1}\right)^{1/(\gamma-1)}d, \tag{4}$$

giving $X_q\approx40d\approx20$ mm for pure He. Similarly, for CS_2 we find $X_q\approx72$ mm. We can reasonably assume that the expansion is incomplete in our interaction region (which is only 3 mm from the nozzle) and, therefore, collisional processes are not yet ''frozen.'' The continuum flow description is valid and the beam properties can be determined by solving the fluid equations using the method of characteristics [17] to give an approximate formula for M. From this, we can find the temperature T through

$$\frac{T}{T_0}=\left(1+\frac{\gamma-1}{2}M^2\right)^{-1}. \tag{5}$$

Although the ratio γ in Eq. (5) refers to a single kind of gas (monatomic, diatomic, or polyatomic), for a gas mixture we can introduce an effective value $\gamma_{\rm eff}$. For an ideal gas mixture the average heat capacity is

$$\overline{C}_p=\sum_i X_i[\gamma_i/(\gamma_i-1)]R, \tag{6}$$

where X_i is the number or mole fraction [17]. As $C_p=\gamma_i/(\gamma_i-1)R$ we can set

$$\overline{C}_p=\frac{\gamma_{\rm eff}}{\gamma_{\rm eff}-1}R. \tag{7}$$

Thus, by equating Eqs. (6) and (7) we have

$$\gamma_{\rm eff}=\frac{\sum_i X_i(\gamma_i/\gamma_i-1)}{\left[\sum_i X_i(\gamma_i/\gamma_i-1)\right]-1}. \tag{8}$$

In the following discussions, the gas mixture temperatures were calculated by evaluating Eq. (5) using $\gamma_{\rm eff}$ values given by Eq. (8). For example, a He partial pressure of 1400 Torr and a CS_2 partial pressure of 350 Torr give $\gamma_{\rm eff}=1.59$ resulting in a CS_2 temperature ≈10 K in the laser focus.

III. RESULTS

Figure 3 shows the measurement of R as a function of the delay between the aligning and harmonic pump pulses, Δt, for 9th order harmonics in CS_2, H_2, and N_2. Positive values of Δt correspond to the pump pulse arriving after the aligning pulse. For each of the molecular species, alignment directions parallel with and perpendicular to the pump pulse electric-field vector are compared. Measurements were made of the 9th, 11th, 13th, and 15th order harmonics, which

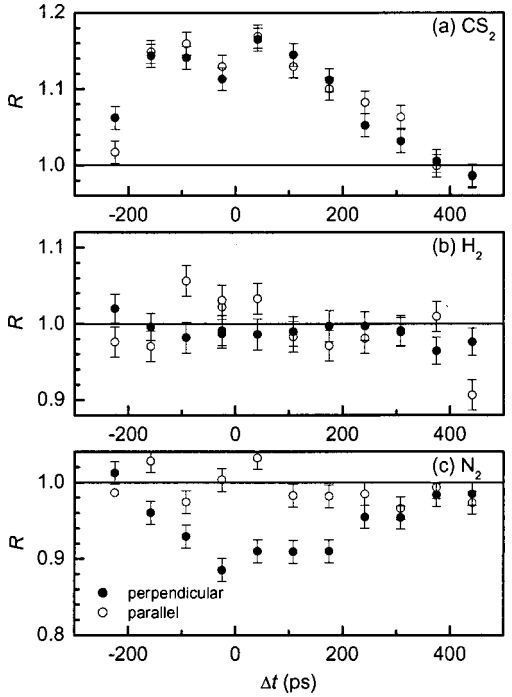

FIG. 3. Ratio R of harmonic intensity with aligning pulse to harmonic intensity without aligning pulse as a function of delay Δt between aligning and harmonic pump pulses for the 9th harmonic using perpendicular (●) and parallel (○) laser polarizations in (a) CS_2, (b) H_2, and (c) N_2.

showed evidence of the same magnitude of alignment effect. We present here only the 9th harmonic ($\lambda = 89$ nm) as it coincides with the peak response of our detection system, resulting in the optimum signal-to-noise ratio.

HHG in CS_2 is enhanced in the presence of an aligning laser pulse [Fig. 3(a)]. The aligning pulse intensity is 2×10^{12} W cm^{-2} and the intensity of the pump pulse is 5×10^{14} W cm^{-2}. The enhancement of R follows the aligning pulse temporal history, although the aligning pulse FWHM duration is 300 ps whereas for R we have a FWHM of $\approx$400 ps. The broadening can be attributed to the nonlinear behavior of R as a function of the aligning pulse intensity (see Fig. 4). There is no significant difference between the parallel and perpendicular polarizations, suggesting that the observed enhancement of HHG is related to the increased order in the aligned molecules and is independent of the alignment direction. We do not expect the aligning pulse to cause significant ionization or dissociation. This is supported by the observation that the aligning pulse has no effect ($R = 1$) when it fully precedes the pump pulse. We observed similar results in hexane, although this molecule was less extensively investigated than CS_2.

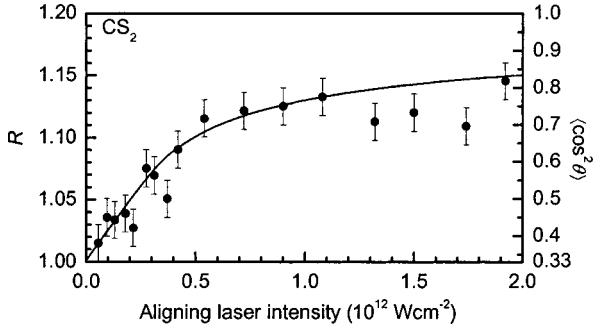

FIG. 4. Ratio R as a function of aligning laser intensity for the 9th harmonic in CS_2 using parallel aligning and pump-laser polarizations.

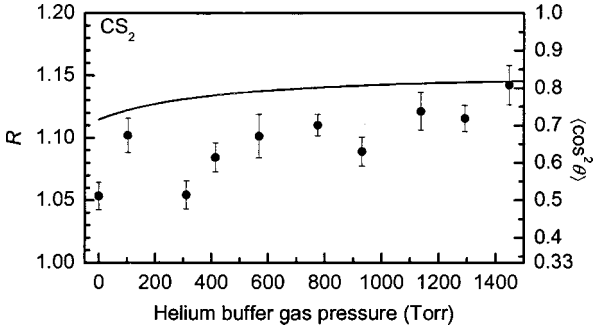

FIG. 5. Filled circles (●) show R for 350-Torr CS_2 as a function of He buffer gas pressure using perpendicular laser polarizations. The continuous curve is the degree of alignment calculated using estimated rotational temperature (25–10 K) and aligning laser intensity (8×10^{11} W cm^{-2}).

No effect is observed in H_2 for either aligning pulse polarization [Fig. 3(b)]. This allows us also to rule out any significant direct influence of the aligning pulse on the harmonic generation process, e.g., through electric-field addition or modified ionization dynamics. Other evidence for this is noted in the dependence of the enhancement effect on pump laser intensity, which shows no decrease in R as the intensity is increased. In N_2 [Fig. 3(c)], prealignment of the molecules perpendicular to the pump pulse causes harmonic emission to be suppressed ($R < 1$), whereas prealignment parallel to the pump pulse has no observable effect. We discuss these results below in terms of the more complicated alignment dynamics of this intermediate mass molecule.

The alignment dependence of HHG in CS_2 is studied as a function of aligning pulse intensity (Fig. 4). The intensity of the harmonic pump pulse is 5×10^{14} W cm^{-2} and its polarization is parallel to that of the aligning pulse. The temporal delay between the two pulses is chosen to maximize R. As the aligning pulse intensity increases from $< 1 \times 10^{11}$ W cm^{-2} to $\sim 5 \times 10^{11}$ W cm^{-2} the harmonic intensity is progressively enhanced ($R > 1$). The effect then saturates and R increases only gradually up to the maximum aligning pulse intensity of 2×10^{12} W cm^{-2}. In the same figure we also show the predicted degree of molecular alignment, $\langle \cos^2 \theta \rangle$, calculated using the formula reported in [13]. The measured variation of HHG and the calculated degree of alignment are strongly correlated.

Further evidence for alignment is presented in Fig. 5, which shows the influence of the He buffer gas pressure on the enhancement factor R. The harmonic pump pulse intensity is 7×10^{14} W cm^{-2} and its polarization is perpendicular to that of the aligning pulse, which has an intensity of $\sim 8 \times 10^{11}$ W cm^{-2}. The effect of the aligning pulse is optimized when the rotational temperature is decreased by maximizing

TABLE I. Molecular properties important to alignment dynamics—moment of inertia, polarizability anisotropy, and rotational constant.

Molecule	$I\,(10^{-45}\ \mathrm{kg\,m^2})$ [18]	$\alpha_\parallel-\alpha_\perp$ (Å^3) [19]	$B\ (\mathrm{cm^{-1}})$ [18]
CS_2	2.56	9.6	0.109
N_2	0.139	0.93	2.0
H_2	0.004 57	0.22	60.9

the buffer gas pressure. Although the rotational temperature can be reduced further by increasing the distance from the nozzle throat to the laser focus, the decreasing density causes a rapid reduction in harmonic intensity resulting in an unfavorable signal-to-noise ratio.

IV. DISCUSSION

To explain these observations we must consider a number of factors: the degree of steady-state alignment caused by the aligning field, realignment of the molecules by the more intense but shorter duration HHG pump pulse and the effect of alignment on the HHG process itself.

A. Degree of alignment and alignment dynamics

The alignment dynamics will be in the adiabatic limit if the laser-pulse duration exceeds the rotational time T_R. In our experiment this condition is always satisfied by the 300 ps duration aligning pulse, as the highest T_R, corresponding to the lowest rotational energy, is $\approx$100 ps for CS_2, 5 ps for N_2, and 0.2 ps for H_2. Table I summarizes the physical properties of these three molecules that are relevant to their alignment dynamics. We evaluate $\langle\cos^2\theta\rangle$ using our predicted rotational temperatures to estimate the degree of alignment induced by an aligning pulse with intensity $2\times10^{12}\ \mathrm{W\,cm^{-2}}$. We find $\langle\cos^2\theta\rangle\approx0.82$ for CS_2, 0.38 for N_2, and 0.33 for H_2. Thus, the aligning pulse produces strong alignment in CS_2 and poor alignment in N_2. In H_2 there is no alignment at all and so this molecule represents the null case (no prealignment).

The subsequent high-intensity, ultrashort pump pulse can also influence the alignment of molecules. It has been shown experimentally that the molecular moment of inertia plays a crucial role in alignment with short pulses. In particular, H_2 and N_2 are forced into alignment by sub-100-fs laser pulses ($I\sim2\times10^{14}\ \mathrm{W\,cm^{-2}}$) whereas under the same conditions, I_2 shows no signs of reorientation [20]. The same conclusion for I_2 is reached with higher-intensity ($10^{15}\ \mathrm{W\,cm^{-2}}$), shorter duration (80 fs) pulses [21]. We can assume that no significant reorientation of CS_2 occurs during the pump pulse. The CS_2 rotational constant is only three times that of I_2 whereas this factor is $\approx$54 for N_2 and $\approx$1600 for H_2. In CS_2 we have observed no dependence of R on the pump pulse intensity, which would be expected if aligning effects of the pump pulse were significant.

H_2 is not oriented by the aligning pulse. This independence from the aligning pulse ensures that H_2 provides a reliable control case for these experiments. This status is not invalidated by the possibility that it may be subsequently aligned by the pump pulse [20].

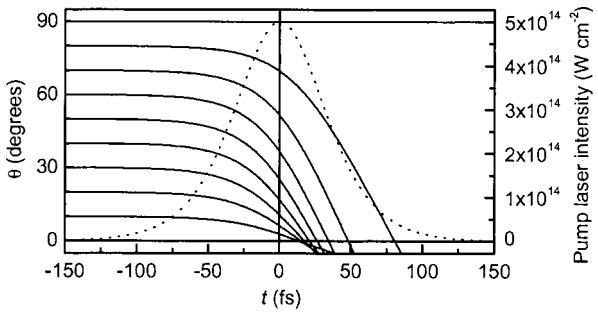

FIG. 6. Realignment of N_2 during a 75-fs harmonic pump pulse. Solid curves are solutions of Eq. (9) for initial alignment angles from 10° to 90°. Dotted curve is the pump pulse intensity. Smaller initial angles result in greater realignment at the peak of the pulse.

It has been shown [20,21] that N_2 undergoes realignment during an intense short pulse. Additionally, we have shown that in our experimental conditions alignment in N_2, though weak, is predicted due to the long pulse. Thus, when using N_2 we have a system that is weakly aligned by the long pulse and subsequently interacts with an intense short pulse. The second pulse is, in turn, able to modify the alignment of the molecular axes. The results for this system are shown in Fig. 3(c) where the measurement of R as a function of the delay between the two laser beams is reported. We see that the prealignment has no effect if realized parallel to the subsequent short harmonic pump pulse whereas it produces a suppression of the harmonic signal if the molecules are preferentially aligned perpendicular to the pump.

To understand such asymmetric behavior we can describe the interaction of N_2 with a short pulse by means of a classical approach valid in the strong-field limit [22,23]. We can neglect the thermal energy with respect to the potential well generated by the short laser pulse and the induced electric dipole, and the differential equation governing the dynamics of the molecule becomes [22]

$$\frac{d^2\theta}{d\tau^2}+\frac{1}{2}\left(\frac{\omega_0}{\omega}\right)^2 g(\tau)\cos^2\tau\sin(2\theta)=0. \tag{9}$$

In Eq. (9) ω is the laser angular frequency, $\tau=\omega t$ is a dimensionless time, $g(\tau)$ is the temporal laser profile, and $\omega_0^2=0.5(\alpha_\parallel-\alpha_\perp)E_0^2/I$, where I is the moment of inertia of the molecule. The initial conditions are $\theta(-\infty)=\theta_0$ and $\dot{\theta}(-\infty)=0$. The latter condition is that the molecule rotational velocity is negligible, which holds also during the adiabatic interaction with the long pulse. The distribution of θ_0 will follow the law $0.5\sin\theta$ (θ ranging in the interval $[-\pi/2,\pi/2]$) if the molecular axes are isotropically oriented. Experimentally, this is the case for H_2 as it is unaffected by the long aligning pulse.

Solutions of Eq. (9) are shown in Fig. 6 for N_2 with $\theta_0=10°-90°$ in 10° increments. We have assumed a sech^2 laser pulse shape with FWHM duration of 75 fs and peak intensity $I_0=5\times10^{14}\ \mathrm{W\,cm^{-2}}$. From Fig. 6 it is evident that the behavior of $\theta(t)$ strongly depends on the initial align-

ment angle θ_0. In particular, this means that small changes in the distribution of θ_0 can lead to large changes in the distribution of $\theta(t=0)$ at the peak of the short pulse when harmonic emission is greatest. Thus, the behavior observed with N_2 can be explained by considering that when the molecule is prealigned parallel to the short pulse, the reorientation induced by the short pulse is enhanced, whereas for perpendicular prealignment reorientation is suppressed. However, in the case when the two pulses are parallel this argument implies an enhancement of HHG, which has not been observed. We argue that the main reason for the observed asymmetric behavior lies in the strong nonlinearity of Eq. (9): molecules at small or intermediate initial angles are strongly realigned, whereas molecules at large initial angles undergo little realignment (see Fig. 6). This implies that the reduction of the degree of alignment obtained when the initial distribution is shifted towards $\pi/2$ (perpendicular prealignment) is expected to be more significant than the improvement obtained in the opposite case. In terms of harmonic generation relative to the case of no long aligning pulse, HHG will be reduced more by perpendicular laser polarizations than it will be enhanced by parallel laser polarizations.

In summary, for N_2, we have a system that is initially slightly aligned ($\langle\cos^2\theta\rangle \approx 0.38$) and subsequently realigned by the ultrashort harmonic pump pulse. The dynamics of the molecule in the potential well generated by the ultrashort laser pulse and the induced electric dipole are strongly nonlinear [22]. In particular, the dynamics of the angle $\theta(t)$ between the molecular axis and the laser electric-field vector strongly depends upon the initial angle θ_0. This means that a small difference in the initial distribution of θ_0 can lead to a very different distribution of $\theta(t=0)$, at the peak of harmonic emission. The behavior observed with N_2 is explained by considering that realignment induced by the pump pulse is assisted when the aligning pulse is polarized parallel to the pump pulse, whereas for perpendicular polarization, reorientation is impeded and so the harmonic intensity is reduced.

B. Enhanced harmonic yield for aligned ensemble of molecules

As stated above, our measurements for CS_2 are consistent with HHG efficiency depending on the degree of alignment but not on the direction of alignment. In earlier theoretical work the direction of alignment was important, but in these calculations the effects of the process on phase matching were not considered [7]. To explain this behavior we invoke a dependence upon molecular alignment of the dipole phase relative to the strong driving field. In the semiclassical picture of HHG, this corresponds to the anisotropy of the molecule leading to different classical trajectories depending upon the direction along which the electron is emitted.

A harmonic wave generated by an atom in the presence of a laser field is shifted in phase with respect to the fundamental wave. This phase shift is equal to the phase of the atomic dipole moment induced by an electromagnetic field. The dependence of such a phase on the laser intensity has been discussed in a number of papers (e.g., [24,25]). In particular, it has been shown that in the semiclassical approach, apart from a small correction, the dipole phase is given by [25]

$$\varphi_{\mathrm{dip}} = \frac{S}{\hbar} \approx \frac{(U_p + I_p)\tau_s}{\hbar}. \tag{10}$$

In Eq. (10), U_p is the ponderomotive potential, S is the quasiclassical action describing the motion of the electron, I_p is the ionization potential, and τ_s is the so-called return time, i.e., the time for the electron to recollide with the nucleus after it tunnels out. In the plateau region, τ_s is approximately one period of the fundamental wavelength [24]. This can lead to a significant phase shift. For example, with $\lambda = 800$ nm, $U_p = 30$ eV ($I = 5\times10^{14}$ W cm^{-2}), and $I_p = 10$ eV we have $\varphi_{\mathrm{dip}} \approx 120$ rad.

In an anisotropic system, such as a linear molecule, we expect φ_{dip} to depend upon the relative orientation of the molecular axis and the electric-field vector of the fundamental beam. In the semiclassical approach, the action depends upon the details of the binding potential through I_p [25]. In a molecule, this factor is orientation dependent. On the other hand, the return time as well as the tunneling time depend upon the atomic binding potential. Thus, it is reasonable to expect that in an anisotropic system the numerator of Eq. (10) will show a dependence upon the direction considered. In our conditions, $\varphi_{\mathrm{dip}} \approx 120$ rad and we see that a change as small as 1% in the numerator of Eq. (10) leads to a change of 1 rad in φ_{dip}.

Once we assume an orientation dependence of the phase of the emitted harmonic [i.e., $\varphi \equiv \varphi(\theta)$], the intensity of the given harmonic will include contributions from all possible molecular orientations. This means that the measured intensity will depend upon the distribution of molecular orientations in the ensemble. In particular, φ is equal for all emitters when all the molecules are aligned in a particular direction (whatever it is). This leads to an enhancement of HHG compared to other distributions (e.g., isotropic). Thus, we suggest that the increase of R we have observed with CS_2 can be ascribed to a reduced angular distribution of the molecular axes.

C. Numerical model of anisotropic behavior

To examine the dependence of the harmonic phase on molecular orientation, we report the results of numerical calculations for a two-dimensional H_2^+ model system. The Hamiltonian for this system in a field $E(t)$ polarized along the x axis is (in atomic units)

$$H = \frac{\mathbf{P}^2}{2} - \sum_{k=1,2} \frac{1}{\sqrt{(x-x_k)^2 + (y-y_k)^2 + 0.5}} + p_x A(t), \tag{11}$$

where $A(t) = -\int_0^t E(t')dt'$, and (x_1, y_1), (x_2, y_2) are the positions of the nuclei. In Eq. (11), a soft Coulomb potential with a smoothing parameter of 0.5 has been used to reproduce the ground-state energy of -30 eV. The time-dependent Schrödinger equation is solved by means of the split-operator method [26]. The amplitude and phase for a har-

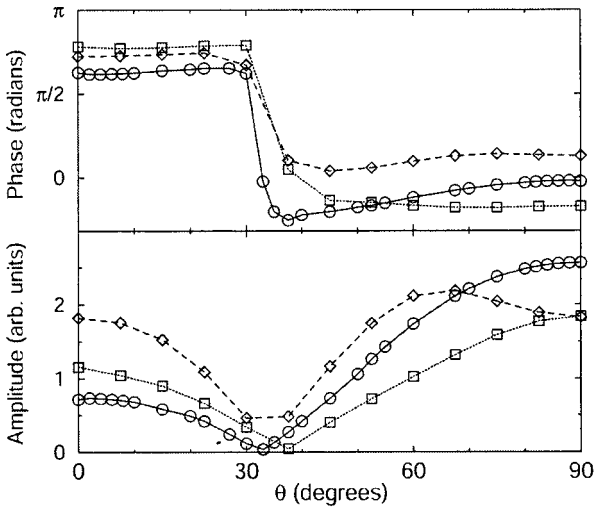

FIG. 7. Harmonic phase and amplitude for the 31st harmonic in the H_2^+ model system as a function of alignment direction. The laser intensities are 5×10^{14} W cm^{-2} (○), 7×10^{14} W cm^{-2} (□), and 1×10^{15} W cm^{-2} (◇).

monic of frequency ω is obtained as the modulus and phase of the complex Fourier transform of the dipole acceleration expectation value [27–29]

$$a(\omega)=\int \langle\Psi(t)|\partial_z V+E(t)|\Psi(t)\rangle e^{i\omega t}dt, \qquad (12)$$

where V is the potential [second term in Eq. (11)]. Equation (12) is for harmonics polarized along the x axis, i.e., parallel to the laser. For symmetry reasons, the yield of harmonics polarized perpendicular to the laser is zero in an ensemble of randomly oriented molecules. The same is true if the molecules are aligned parallel or perpendicular to the laser as in the present experiment. In the calculation we employ laser pulses of 780 nm wavelength and a total duration of ten optical cycles (26 fs). The field is switched on and off using three-cycle linear ramps.

The positions of the nuclei are fixed, so realignment by the short harmonic pump pulse is not possible. In this respect, these calculations are most closely related to the experimental results for CS_2, the heaviest molecule investigated. The calculated harmonic phase cannot be directly compared to Eq. (10) since it is found by taking the phase of the complex value $a(\omega)$ and is, therefore, only defined modulo 2π.

Figure 7 displays the calculated orientation dependence of the phase and amplitude for the 31st harmonic. The 31st order has been chosen because the ionization potential of H_2^+ is three times as large as that of CS_2. Since the harmonics considered in the present experiment correspond to transitions from electronic energy levels not far above the ionization potential, it is appropriate to scale the harmonic frequencies by multiplying by the ratio between the ionization potentials. In this sense, the 31st harmonic in H_2^+ corresponds to the 9th or 11th harmonic in CS_2. Three different laser intensities have been employed: 5×10^{14} W cm^{-2}, 7×10^{14} W cm^{-2}, and 1×10^{15} W cm^{-2}. For all three intensities, we observe the same phenomenon: the phase depends weakly on the angle of alignment except for a sudden jump at a certain critical angle. The size of the phase jump is in the vicinity of π. The critical angle is the same for all three intensities. The amplitude is at a local minimum at the same angle. A detailed investigation of this effect that is also found for most other high harmonics will be published elsewhere. In this paper, we concentrate on comparing the harmonic yield of aligned molecules to that of randomly oriented molecules. In the latter case, we must sum the complex contributions, Eq. (12), of all angles between 0° and 90°, weighted by their respective solid angle factors. The result for the laser intensity 5×10^{14} W cm^{-2} is shown in Fig. 8. Here, we have plotted the ratio between aligned and random orientation for alignment angles of 0° and 90°. In the intermediate range of harmonics (orders 9–37), our results show the same trend that was already found for higher intensities [7]: harmonic generation is more effective in perpendicular alignment than in parallel alignment. In this regime, the summation over all angles leads to a harmonic yield lying in between those for 0° and 90°. Apparently, the contributions of orientations close to 90° are dominant through their larger amplitudes. For higher orders, the difference between parallel and perpendicular alignment is small. Here, the yield of randomly oriented molecules is smaller by a factor that ranges between 1 and 60. Such a strong suppression cannot be explained in terms of the harmonic amplitudes only. Rather, the orientation dependence of the phase leads to a destructive interference between the contributions from angles close to 0° and those close to 90°. This agrees well with the experimental results for CS_2, where parallel and perpendicular alignment are found to give similar yields, and for no alignment the yield is smaller.

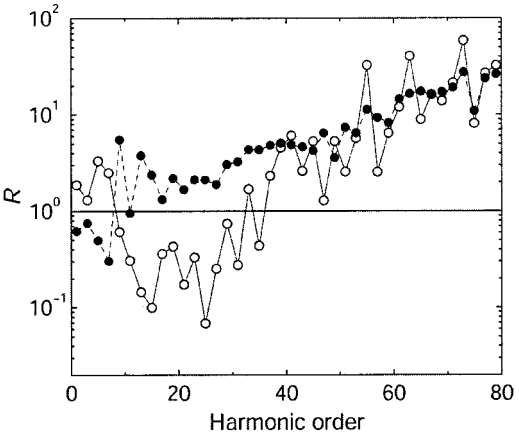

FIG. 8. Calculated R versus harmonic order in the H_2^+ model system. The alignment is perpendicular (●) or parallel (○) to the pump-laser polarization. The laser intensity is 5×10^{14} W cm^{-2}.

V. CONCLUSIONS

In conclusion, we have made an experimental observation of an alignment dependence of HHG in molecules. This required us to demonstrate, for the first time to our knowledge, molecular alignment in a dense vapor ($\sim10^{17}$ cm^{-3}) corre-

sponding to $\sim 10^{13}$ molecules in the laser focus. We propose an explanation for the alignment dependence in terms of an anisotropic intensity-dependent dipole phase. Enhanced HHG is found in aligned molecular systems and this may have implications for future developments of this unique light source. Moreover, studies of the harmonic response of aligned molecules provide a powerful tool for the understanding of anisotropic molecular electron dynamics in intense fields.

This method of controlling HHG should be common to all molecules, such as CS_2 and hexane, for which controllable alignment can be produced with adiabatic pulses of intensity $\sim 10^{12}$ W cm^{-2}. Investigation of these effects in other species is now underway. We note that modulation of the harmonic yield by controlled molecular alignment may also permit exploitation in a scheme for enhanced HHG using quasiphase matching [30].

ACKNOWLEDGMENTS

We gratefully acknowledge the contributions of J. W. G. Tisch, M. B. Mason, K. J. Mendham, and M. H. R. Hutchinson, the technical assistance of P. Ruthven and A. Gregory, and useful discussions with H. Stapelfeldt. This work was supported by the UK EPSRC, by EC-IHP (Grant Nos. HPMF-CT-1999-00346 and HPRN-CT-1999-00129), and by a British Council-Ministerio de Educación y Cultura (MEC, Spain) Acción Integrada.

[1] P. Salières *et al.*, Adv. At., Mol., Opt. Phys. **41**, 83 (1999).
[2] P. B. Corkum, Phys. Rev. Lett. **71**, 1994 (1993).
[3] Y. Liang *et al.*, J. Phys. B **27**, 5119 (1994).
[4] C. Lyngå, A. L'Huillier, and C.-G. Wahlström, J. Phys. B **29**, 3293 (1996).
[5] N. Hay *et al.*, Phys. Rev. A **62**, 041803 (2000).
[6] M. Plummer and J. F. McCann, J. Phys. B **30**, L401 (1997).
[7] D. G. Lappas and J. P. Marangos, J. Phys. B **33**, 4679 (2000).
[8] R. Velotta *et al.*, Phys. Rev. Lett. **87**, 183901 (2001).
[9] M. Lein *et al.* Phys. Rev. Lett. (to be published).
[10] J. J. Larsen *et al.*, J. Chem. Phys. **111**, 7774 (1999).
[11] W. Kim and P. M. Felker, J. Chem. Phys. **104**, 1147 (1996).
[12] R. W. Boyd, *Nonlinear Optics* (Academic, London, 1992).
[13] B. Friedrich and D. Herschbach, Phys. Rev. Lett. **74**, 4623 (1995); J. Phys. Chem. **99**, 15 686 (1995).
[14] J. J. Larsen *et al.*, J. Chem. Phys. **109**, 8857 (1998).
[15] H. Sakai *et al.*, J. Chem. Phys. **110**, 10 235 (1999).
[16] J. J. Larsen, I. Wendt-Larsen, and H. Stapelfeldt, Phys. Rev. Lett. **83**, 1123 (1999).
[17] D. R. Miller, in *Atomic and Molecular Beam Methods*, edited by G. Scoles (Oxford University Press, New York, 1988), Vol. 1.
[18] A. M. James and M. P. Lord, *Macmillan's Chemical and Physical Data* (MacMillan, London, 1992).
[19] J. O. Hirschfelder, C. F. Curtis, and R. B. Bird, *Molecular Theory of Gases and Liquids* (Wiley, New York, 1954).
[20] J. H. Posthumus *et al.*, J. Phys. B **31**, L553 (1998).
[21] C. Ellert *et al.*, Philos. Trans. R. Soc. London, Ser. A **356**, 329 (1998).
[22] M. E. Sukharev and V. P. Kraĭnov, JETP **86**, 318 (1998).
[23] B. A. Zon, Eur. Phys. J. D **8**, 377 (2000).
[24] M. Lewenstein, P. Salières, and A. L'Huillier, Phys. Rev. A **52**, 4747 (1995).
[25] M. Lewenstein *et al.*, Phys. Rev. A **49**, 2117 (1994).
[26] M. D. Feit, J. A. Fleck Jr., and A. Steiger, J. Comput. Phys. **47**, 412 (1982).
[27] B. Sundaram and P. W. Milonni, Phys. Rev. A **41**, 6571 (1990).
[28] J. H. Eberly and M. V. Fedorov, Phys. Rev. A **45**, 4706 (1992).
[29] D. G. Lappas, M. V. Fedorov, and J. H. Eberly, Phys. Rev. A **47**, 1327 (1993).
[30] R. L. Byer, J. Nonlinear Opt. Phys. Mater. **6**, 549 (1997).